ARTICLE NO. 79-0211R

C80-023

Dynamic Stall at High Frequency and Large Amplitude

00001
20009

Lars E. Ericsson* and J. Peter Reding†
Lockheed Missiles & Space Company, Inc., Sunnyvale, Calif.

A previously developed quasisteady analytic method has been shown to give predictions that are in good agreement with experimental stall results as long as the oscillation amplitude and frequency are of moderate magnitudes. In the present paper, this quasisteady method is extended to include the transient effect of the "spilled" leading-edge vortex, thereby providing simple analytic means for prediction of dynamic stall characteristics at high frequency and large amplitudes. The veracity of the method is demonstrated by critical comparisons with the extensive experiments performed by Carr et al.

Nomenclature

c = two-dimensional chord length
K_a = dynamic overshoot coefficient, Eq. (2)
l = section lift, coefficient $c_l = l/(\rho_\infty U_\infty^2/2)c$
m_p = section pitching moment, coefficient $c_m = m_p/(\rho_\infty U_\infty^2/2)c^2$
n = section normal force, coefficient $c_n = n/(\rho_\infty U_\infty^2/2)c$
t = time
U = velocity
x = chordwise distance from the leading edge
z = vertical translation
α = angle of attack
α_0 = trim angle of attack
Γ = circulation
Δ = increment
θ = angle-of-attack perturbation
ξ = dimensionless x coordinate, $\xi = x/c$
ξ_{CG} = center of oscillation
ρ = air density
φ_w = wake lag
φ_s = stall-induced additional phase lag
$\omega, \bar{\omega}$ = oscillation frequency, $\bar{\omega} = \omega c/U_\infty$

Subscripts

c = convection
CG = center of gravity
DYN = dynamic
eff = effective
LE = leading edge
lg = linear growth
max = maximum
QS = quasisteady
s = stall
sp = separation point movement
TE = trailing edge
tot = total
v = vortex
vg = vortex growth
vs = vortex spillage
w = wake and wall
∞ = undisturbed flow

Superscripts

i = induced and inducing, e.g., α^i = separation inducing angle of attack
$(-)$ = mean value

Presented as Paper 79-0211 at the AIAA 17th Aerospace Sciences Meeting, New Orleans, La., Jan. 15-17, 1979; submitted Feb. 13, 1979; revision received Aug. 13, 1979.

Index categories: Nonsteady Aerodynamics; Aerodynamics.

*Consulting Engineer. Associate Fellow AIAA.
†Research Specialist. Member AIAA.

Introduction

SINCE the classical investigation by Halfman et al.,[1] the dynamic stall problem has been studied intensively. Although our understanding of the basic flow phenomena has improved greatly as a result, no substantial advancement of our capability to predict dynamic stall characteristics has resulted. On the one hand, it is difficult to use subscale test data because of the problem of dynamic simulation,[2] especially in the presence of three-dimensional flow effects in so-called "two-dimensional" dynamic stall tests.[3,4] On the other hand, no pure theory exists that can predict the dynamic overshoot of static stall[5,6] or the dynamic overshoot of static reattachment. It will be quite some time before pure theory can predict all the details in the oscillatory dynamic stall cycle leading to negative aerodynamic damping and associated stall flutter. It will also be a while before simulation of full-scale dynamics in subscale tests becomes routine.[7]

An earlier developed analytic method[8,9] has been shown to predict numerical and experiment results as long as the reduced frequencies and oscillation amplitudes are of modest magnitudes.[10] In order to provide an analytic method that can predict the dynamic stall characteristics also when the oscillation amplitude is large and the reduced frequency is high, the transient effect of the "spilled" leading edge vortex has to be considered.[11,12] The extensive, systematic experiments performed by Carr et al.[13] indicated that other modifications of the quasisteady theory also were needed. The present paper describes these modifications. To make the analysis easier to follow, the salient parts of the quasisteady method[8,10] will be recapitulated.

Analysis

The present method is semiempirical in nature. It uses static experimental data as an input. In addition, certain critical proportionality constants for the effects of pitch amplitude and frequency on the unsteady separation process have been determined by use of dynamic experimental data.

Quasisteady Analysis

In the analysis it is postulated that the quasisteady overshoot of static $c_{l\max}$ is caused by the following dynamic effects on the boundary layer: 1) boundary-layer improvement due to pitch-rate-induced upstream pressure gradient relief; and 2)

boundary-layer improvement caused by the leading edge plunging, the so-called "leading edge jet" effect. It is postulated further that the upper boundary for this dynamic improvement of the boundary layer is the static infinite Reynolds number limit. Thus, the quasisteady overshoot of static $c_{l\max}$, expressed in the form of an increase of the stall angle, is $c_{l_\alpha} \cdot \Delta\alpha_s$, where $\Delta\alpha_s$ has the following components:

$$\begin{aligned} \Delta\alpha_s &= \Delta\alpha_{s1} + \Delta\alpha_{s2} \le (\Delta\alpha_s)_{\max} \\ \Delta\alpha_{s1} &= K_{a1}(c\dot{\alpha}/U_\infty) \\ \Delta\alpha_{s2} &= -K_{a2}(\dot{z}_{LE}/U_\infty) \end{aligned} \tag{1}$$

For an airfoil pitching around ξ_{CG}, one has

$$\begin{aligned} \Delta\alpha_s &= K_a c\dot{\alpha}/U_\infty \le (\Delta\alpha_s)_{\max} \\ K_a &= K_{a1} + K_{a2}\xi_{CG} \end{aligned} \tag{2}$$

For the analysis to date, which has been concerned largely with the NACA-0012 airfoil, $K_{a1} = 2$ and $K_{a2} = 4$; that is, $K_a = 3$ for $\xi_{CG} = 0.25$.‡ It is also assumed that $(\Delta\alpha_s)_{\max} = 0.02 K_a$ based upon dynamic experimental data.[14]

In addition to this dynamic overshoot, $c_{l_\alpha}\Delta\alpha_s$, of static lift maximum, there is an overshoot $\Delta\alpha$ due to pure time lag effects which causes no corresponding overshoot of static lift maximum. One contribution to this lag is the Karman-Sears circulation lag.[15] It was shown in Ref. 8 that this wake lag effect could be approximated as follows for an airfoil oscillating in pitch.

$$\begin{aligned} \Delta^i(t) &= \alpha_0 + \Delta\theta\sin(\omega t - \varphi_w) \\ \varphi_w &= \begin{cases} 1.5\omega: & \bar{\omega} \le 0.16 \\ 0.245: & \bar{\omega} > 0.16 \end{cases} \end{aligned} \tag{3}$$

That is, $\Delta\alpha_w = \Delta\theta\sin\phi_w$.

For a rampwise α change, the lag effect is:

$$\Delta\alpha_w = 1.5c\dot{\alpha}/U_\infty \tag{4}$$

In the engineering analysis to date,[8-10] it has been assumed that Eq. (3) could be applied also when oscillating into the stall region. The experimental data by Carr et al.[13] show that this is a bad assumption. Figure 1 illustrates why. When oscillating through stall, the vortex wake does not have the continuously changing sinusoidal shape typical for attached flow (Fig. 1a), but rather resembles that of an airfoil describing a series of α ramps (Fig. 1b). Thus, in the present analysis, φ_w is described by Eq. (3) only for completely attached flow. For oscillations into the separated flow region, the constant time lag approximation is applied also for $\omega > 0.16$.

$$\varphi_w = 1.5\omega \tag{5}$$

Another contribution to the lag term ($\Delta\alpha$), the boundary layer convection lag ($\Delta\alpha_c$), which is important for trailing edge stall, e.g., due to shock-induced boundary-layer separation,[16] is of little importance when dealing with leading edge stall, which is the stall type dealt with in this paper, except when expressly stated otherwise.

Transient Effects

When the static stall angle α_s has been exceeded by $\Delta\alpha_s + \Delta\alpha$, separation occurs on the oscillating airfoil and the following transient events take place. The separation point moves toward the leading edge and a leading-edge vortex is "spilled." If the airfoil is describing oscillations in pitch, $\theta(t) = \Delta\theta\sin(\omega t)$, around α_0, the phase angle $(\omega t)_{vs}$ for the vortex spillage can be obtained as follows by use of Eq. (2).

$$\alpha_0 + \Delta\theta\sin[(\omega t)_{vs} - \varphi_w - \varphi_s] = \alpha_s + \Delta\alpha_s$$

$$\Delta\alpha_s = \begin{cases} K_a\Delta\theta\bar{\omega}\cos(\omega t)_{vs}: & \bar{\omega}\Delta\theta\cos(\omega t) < 0.02 \\ (\Delta\alpha_s)_{\max} = 0.02K_a: & \bar{\omega}\Delta\theta\cos(\omega t) \ge 0.02 \end{cases}$$

$$\varphi_w = 1.5\bar{\omega} \qquad \varphi_s = \xi_{sp}\bar{\omega}$$

$$\xi_{sp} = \begin{cases} 0.75: & \text{turbulent separation} \\ 3.0: & \text{laminar separation} \end{cases}$$

$$K_a = 2(1 + 2\xi_{CG}) \tag{6}$$

Solving for $(\omega t)_{vs}$ in Eq. (6) gives:
For $\omega\Delta\theta\cos(\omega t)_{vs} < 0.02$,

$$(\omega t)_{vs} = 2\tan^{-1}\left[\frac{\cos(\varphi_w + \varphi_s)}{K_a\bar{\omega} + \sin(\varphi_w + \varphi_s) + (\alpha_0 - \alpha_s)/\Delta\theta}\right] \times \left\{\sqrt{1 + \frac{[K_a\bar{\omega} + \sin(\varphi_w + \varphi_s)]^2 - [(\alpha_0 - \alpha_s)/\Delta\theta]^2}{\cos^2(\varphi_w + \varphi_s)}} - 1\right\} \tag{7a}$$

For $\bar{\omega}\Delta\theta\cos(\omega t)_{vs} \ge 0.02$,

$$(\omega t)_{vs} = \varphi_w + \varphi_s + \sin^{-1}\left(\frac{0.02K_a + \alpha_s - \alpha_0}{\Delta\theta}\right) \tag{7b}$$

According to measurements,[17,18] the "spilled" leading-edge vortex travels down the chord with an average velocity $\bar{U}_v \approx 0.55U_\infty$. The phase lag, $(\Delta\omega t)_{vTE}$, corresponding to the time needed for the vortex to travel from the leading edge to the trailing edge is:

$$(\Delta\omega t)_{vTE} = (U_\infty/\bar{U}_v)\bar{\omega} = 1.8\omega \tag{8}$$

Equation (6) shows that it makes a big difference whether the leading-edge separation is laminar or turbulent. In the static case, the separation is definitely laminar. It was long assumed that the dynamic leading edge stall also was laminar. It has been suggested earlier[19] that the dynamic leading-edge jet effect[9,19] could be very similar to the effect observed by Hurley and Ward,[20] of airjets in the leading-edge region. Hurley showed that by applying minute blowing rates in the region between stagnation and separation points, the laminar leading-edge bubble could be eliminated completely. McCroskey et al.[21] recently published dynamic experimental results that demonstrated that the laminar separation bubble did indeed disappear and that dynamic leading-edge stall is turbulent in nature, at least for the NACA-0012 airfoil.

Figure 2 shows how this change from $\xi_s = 3.0$ to $\xi_s = 0.75$, together with the change of φ_w discussed earlier, dramatically changes the prediction of dynamic stall at high frequencies. It should be noted that the predicted upper branch will be lifted in Fig. 2b when the "spilled" vortex effect is included, as will be demonstrated shortly. Figure 2a shows that the lower branch will also be lifted if a modified phase lag is used, in which the moving separation point does not reach its mean velocity instantaneously, but requires a certain time to accelerate to this speed.[22]

Figure 3 shows the results obtained for NACA-0012 by use of Eqs. (6-8). A value of $\alpha_s = 14.5$ deg was obtained from the data in Ref. 13. It can be seen that the agreement between predicted vortex spillage and measured begin moment stall is good. Also, the measured phase lag for moment maximum,

‡Note that for a sharp leading edge, $K_a = 0$.

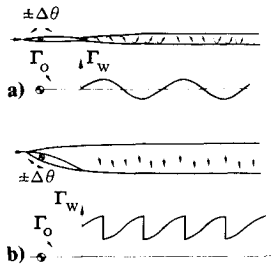

Fig. 1 Unsteady vortex wakes for attached and stalled flow over an airfoil. 2) attached flow; b) dynamic stall.

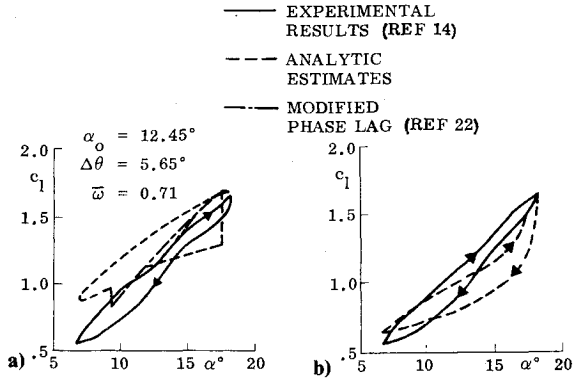

Fig. 2 Predictions of dynamic lift stall loops. a) old method; b) new method.

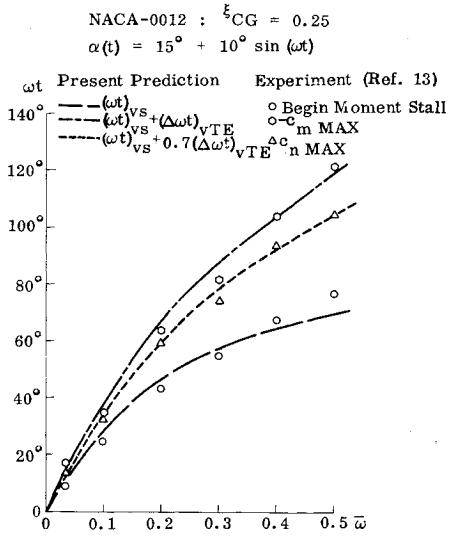

Fig. 3 Predicted and measured dynamic stall phase angles.

$c_{m_{max}}$, is in good agreement with the predicted phase lag for passage of the spilled vortex over the trailing edge. The moment should, of course, peak just before the vortex leaves the airfoil, and c_{nmax} should occur somewhat earlier.[9] The test data in Fig. 3 indicate that the phase lag that should be added to $(\omega t)_{vs}$ to predict the occurrence of c_{nmax} is approximately 70% of $(\Delta\omega t)_{vTE}$. This estimate is shown by the dashed line in Fig. 3.

Figure 4a shows similar results for a cambered airfoil§ for which the static stall angle is $\alpha_s = 16$ deg (see Ref. 13). The results shown in Fig. 4b for an airfoil with a sharp leading edge are, however, quite different. For the sharp leading edge, $K_a = 0$ and $\varphi_s = 0$, as the separation is fixed at the leading edge. For this airfoil, the data in Ref. 13 show $\alpha_s = 12$ deg. The agreement between $(\omega t)_{vs}$ and begin moment stall is

§This airfoil has trailing-edge type stall. However, at $c_{l\,max}$ stall occurs near the leading edge and it is assumed that also for this airfoil $\Delta\alpha_c \approx 0$ and $\varphi_s = 0.75\,\bar{\omega}$.

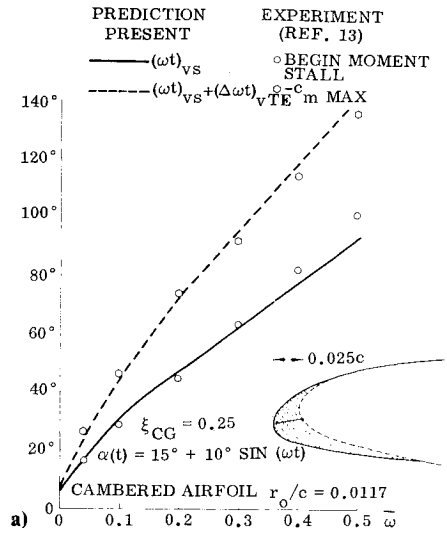

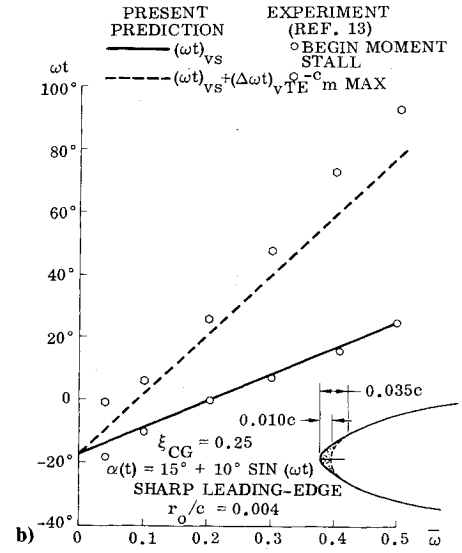

Fig. 4 Effect of profile shape on dynamic stall phase angles. a) cambered airfoil; b) sharp leading-edge airfoil.

good, but it appears that the vortex may travel slower than in the case of the other two airfoils. $\bar{U}_v/U_\infty \approx 0.4$ is indicated rather than $\bar{U}_v/U_\infty \approx 0.55$, the vortex velocity measured on NACA-0012.[17,18] This would be in agreement with the observation made at the test[13] "that the vortex is much more highly coiled and is further forward on the airfoil than that associated with trailing-edge stall" (on the cambered airfoil).

When the amplitude and frequency of the oscillation are of appreciable magnitudes, the "spilled" leading-edge vortex can be seen to have a marked effect on the unsteady stall characteristics[13] (Fig. 5). As the oscillation frequency is increased, the s[illegible]ed vortex effect moves from the upstroke to the downstroke portion of the cycle with associated large effects on the dynamic stall loops. For example, at $\bar{\omega} = 0.3$, the effect on the pitch damping is negligible but becomes highly undamping at $\bar{\omega} = 0.5$. Thus, it is very important to be able to predict the phase angle for the spilled vortex event, a capability demonstrated in Figs. 3 and 4. In addition, one needs to be able to predict the vortex-induced force and moment amplitudes. Previously, the space-time equivalence between the unsteady "spilled" vortex and the stationary vortex on a delta wing has been used to develop the following expression for the vortex-induced normal force.[11,12]

$$\Delta c_{nv} = 1.5\pi \sin^2 \alpha_{vs} \qquad (9)$$

where, for the oscillating airfoil,

$$\alpha_{vs} = \alpha_0 + \Delta\theta \sin(\omega t)_{vs} \tag{10}$$

That this formulation may be an oversimplification was always understood. Both Carta's fluctuating pressure measurement[23] and the flow visualization results obtained by Silcox and Szwarc[24] indicate that the vortex is not "spilled" from the leading edge directly, but first spends some time near the leading edge growing in size. Carta's data[23] suggest that the vortex moves from the leading edge to 25% chord with half the mean vortex velocity; i.e., $\bar{U}_{vl} = 0.5\ \bar{U}_v$. The phase angle corresponding to this vortex growth period is $0.9\ \bar{\omega}$. It is, therefore, proposed that Eqs. (9) and (10) be changed as follows:

$$\Delta c_{nv} = 1.5\pi \sin^2 (\alpha_{vs})_{\text{eff}} \tag{11}$$

$$(\alpha_{vs})_{\text{eff}} = \alpha_0 + \Delta\theta \sin[(\omega t)_{vs} + 0.9\bar{\omega}] \tag{12}$$

The expressions for $(c_{n\max})_{\text{DYN}}$ are:

$$(c_{n\max})_{\text{DYN}} = (c_{n\max})_{QS} + (\Delta c_n)_{\text{QS}} + \Delta c_{nv}$$

$$(c_{n\max})_{\text{QS}} = c_{n\alpha}(\alpha_s + \Delta\alpha_s) \tag{13}$$

$$-(c_{m\,\max})_{\text{DYN}} = (c_{n\,\max})_{\text{QS}}(0.25 - \xi_{\text{CG}})$$

$$-(\Delta c_m)_{\text{QS}} - (1 - \xi_{CG})\Delta c_{nv} \tag{14}$$

$(\Delta c_n)_{\text{QS}}$ and $(\Delta c_m)_{\text{QS}}$ are the contributions caused by pitch-rate-induced camber and apparent mass effects.[10,19] They are usually negligibly small compared to the other contributions.

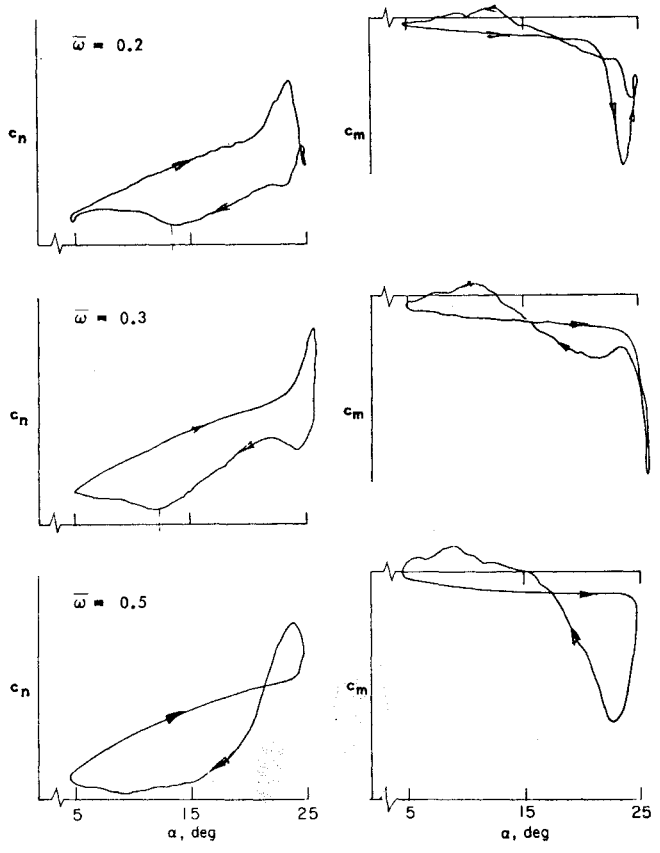

Fig. 5 Dynamic stall loop for the NACA-0012 airfoil oscillating at high frequencies and large amplitude (10 deg) around $\xi_{\text{CG}} = 0.25$ and $\alpha_0 = 15$ deg (Ref. 13).

For the common case that $\xi_{\text{CG}} = 0.25$, Eq. (14) becomes simply

$$-(C_{m\,\max})_{\text{DYN}} = 0.75\Delta c_{nv} - (\Delta c_m)_{\text{QS}} \tag{15}$$

Figure 6 shows that the peak dynamic normal force and moment predicted by Eqs. (13) and (15), respectively, are in reasonable agreement with those measured on a NACA-0012 airfoil at different frequencies.[13] The data uncertainty indicated in Fig. 6 was obtained from Ref. 25. It should be noted that these quantitative results are very different from those given in Ref. 6 for the same test conditions. This data uncertainty is reflected in the fact that no quantitative scales are given in Ref. 13 for c_n or c_m. One source of data uncertainty is the nonrepetivity of the dynamic stall loops.[9,26] Another is the sidewall three-dimensional flow interference,[2-4] which is present in Ref. 13 until $\bar{\omega} \leq 0.3$ according to the authors.

When considering the cambered and sharp leading-edge airfoils, Figs. 7a and 7b, respectively, the comparison is not as good. In addition to the experimental data uncertainty, one has to consider that the parameter values K_a and φ_s of NACA-0012 were used also for the cambered airfoil, and that $K_a = 0$ is a rather crude approximation for the sharp leading-edge airfoil.

Rampwise α-Change

In the case of rampwise α-change, Eq. (6), as amended by Eq. (12), is substituted by Eq. (16) following the procedure outlined in Ref. 10.

$$(\alpha_{vs})_{\text{eff}} = \alpha_s + \Delta\alpha_w + \Delta\alpha_s + \Delta\alpha_{sp} + \Delta\alpha_{vg}$$

$$\Delta\alpha_w = \xi_w c\dot{\alpha}/U_\infty \qquad \Delta\alpha_s = K_a c\dot{\alpha}/U_\infty$$

$$\Delta\alpha_{sp} = \xi_{sp}(c\dot{\alpha}/U_\infty) \qquad \Delta\alpha_{vg} = 0.9(c\dot{\alpha}/U_\infty) \tag{16}$$

Due to the pitch-rate-induced camber and apparent mass effects, the attached flow lift curve will lag the instantaneous angle of attack by only half the Karman-Sears wake lag.[10] Thus, the linear lift growth will stop at the angle

$$\alpha_{lg} = \alpha_s + \Delta\alpha_w/2 + \Delta\alpha_s + \Delta\alpha_{sp} \tag{17}$$

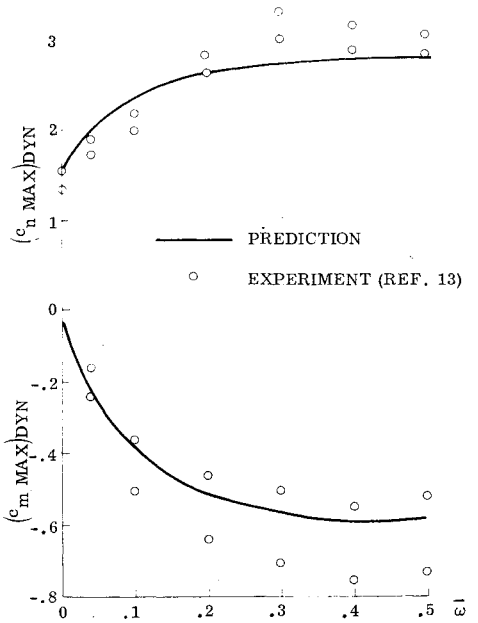

Fig. 6 Maximum dynamic force and moment for the NACA-0012 airfoil.

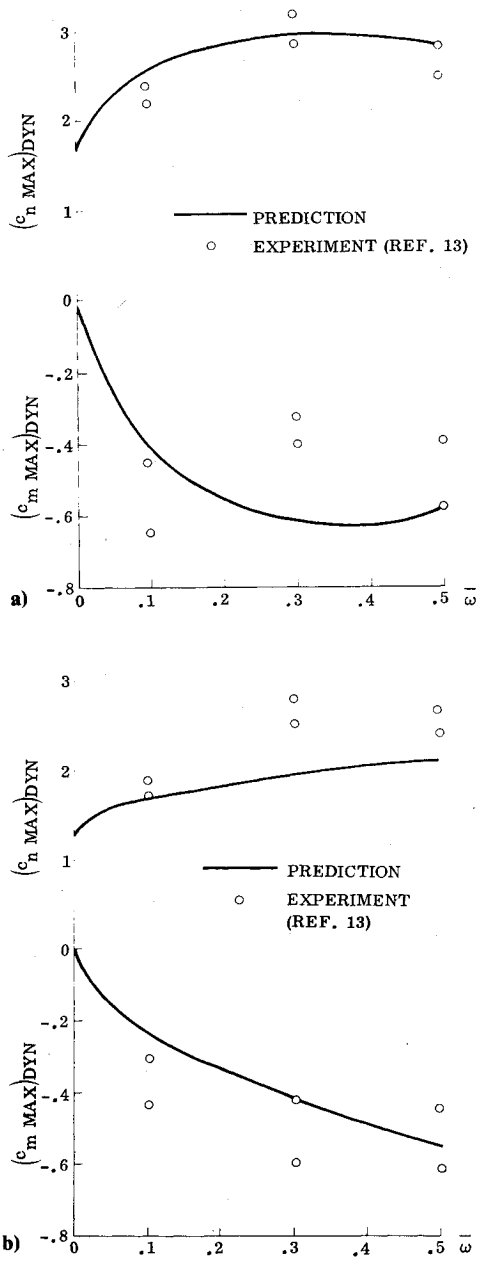

Fig. 7 Effect of airfoil shape on the maximum dynamic force and moment. a) cambered airfoil; b) sharp leading-edge airfoil.

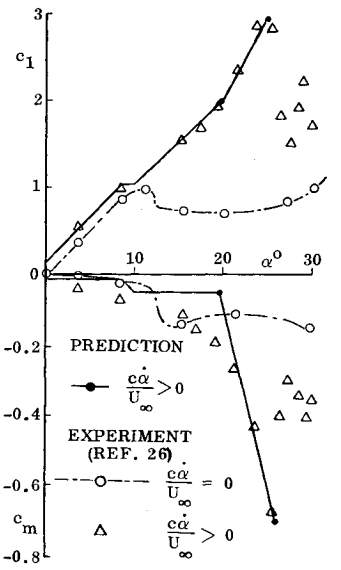

Fig. 8 Comparison of experimental α-ramp results with present predictions.

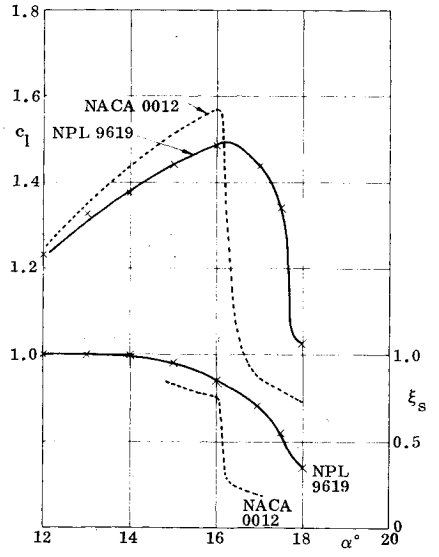

Fig. 9 Static deep stall characteristics (Ref. 3).

Combining Eqs. (11-17) gives the prediction shown in Fig. 8 of the experimental results obtained by Ham and Garelick.[27] The excellent agreement resulted after the predictions had been zero-shifted -2.5 deg to agree with the attached flow lift at low angles of attack. How the attached flow characteristics are obtained is described in detail in Refs. 10-12 and also in Ref. 28. Comparing the present prediction with that in Ref. 12 shows that the introduction of $\Delta\alpha_{vg}$ greatly improves the agreement with experimental results.

The experimental α-ramp data in Fig. 8 exhibit an oscillatory behavior. There is a great similarity between the incompressible stall data obtained by Ham and Garelick[27] and the compressible, shock-induced stall data published by Lambourne.[29] It was shown in Ref. 16 how the unsteady characteristics of the shock-induced separation can be predicted. An equivalent to Eq. (16) determines the magnitude of the first oscillatory overshoot of the static separation point. The correlation between separation point movement and deep stall lift characteristics for NACA-0012 and NPL 9619 (Ref. 3 and Fig. 9) indicates that the analysis of Ref. 16 could probably be extended to predict the incompressible oscillatory α-ramp characteristics shown in Fig. 8. The large amplitude oscillatory tests performed by Carr et al.[13] also produced superimposed oscillations similar to those for the α-ramp, but only for the NACA-0012 and cambered airfoils, not for the sharp leading-edge airfoil (Fig. 10). This is all in agreement with the role played by the moving separation point in these superimposed oscillations. As the sharp leading-edge airfoil has the separation fixed at the leading edge, $\xi_{sp}=0$ as discussed earlier, the large effects of the moving separation point on phase lag and superimposed oscillations are absent (Fig. 10).

With the introduction of the constant time-lag approximation for the deep stall characteristics, Eq. (5), and the vortex growth period $\Delta\alpha_{vg}$ in Eq. (16), the interesting dynamic stall inhibition phenomenon observed by McCroskey and Philippe[30] can be explained. The top part in Fig. 11 shows their data, with the NACA-0012 airfoil oscillating into the stall region without ever realizing lift stall. The bottom part shows the graphic representation of the corresponding phase lag characteristics, presented in Ref. 31. With the old method,[10] the required phase lag, $\varphi_{tot} = 1.1\pi$, for inhibition of stall could not be predicted. The present modified method gives $\varphi_{tot} = 6.15\bar{\omega} = 1.33\pi$, thus predicting the stall inhibition. This high-frequency bonus, the stall inhibition,

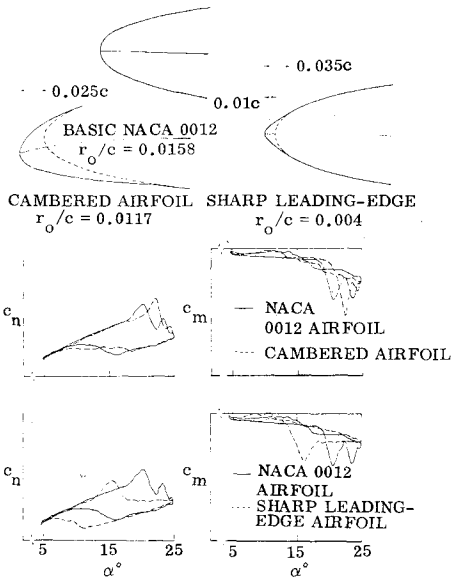

Fig. 10 Stall loops at $\omega = 0.10$ for various airfoil shapes (Ref. 13).

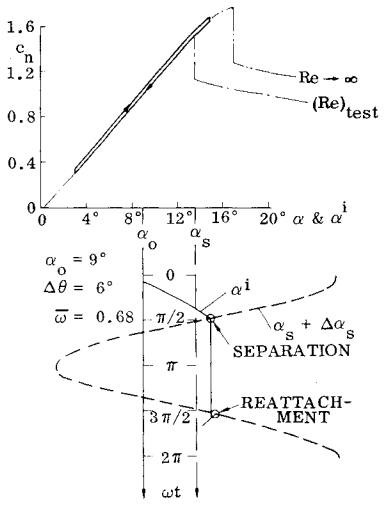

Fig. 11 Dynamic inhibition of the stall (Ref. 31).

has important practical implications for the rotor design of helicopters, windmills, and axial compressors.

The preliminary results obtained so far indicate that the present analytical method, with the improvements made possible by the detailed experiments performed by Carr et al.,[13] can predict existing experimental dynamic stall results. Thus, if the computerized method outlined in Ref. 22 is extended to include all the changes that have occurred since then, described and summarized in the present paper, it should provide a valuable preliminary design tool for the helicopter and compressor industries.

As noted by McCroskey in his most recent review of the existing capability in predicting unsteady separated flows on oscillating airfoils,[32] the present method is the most comprehensive one. It utilizes all available experimental and theoretical information and is, for example, the only one distinguishing between plunging and pitching oscillations. Although the present method in no way obviates basic research into the complex flow phenomena composing dynamic stall, semiempirical methods of this type are the only ones that can provide the engineer with any help for preliminary design, a conclusion also reached by McCroskey.[32] Bore, in his review of our work,[33] goes one step further, pointing out how the simple, explicit flow mechanisms on which our method is based, in addition to helping the vehicle designer to understand dynamic stall, also illuminate the vital flow processes in stall flutter, rapid pull-ups, wing rocking, and buffet.

Conclusions

A renewed look at earlier developed engineering analysis methods for dynamic stall, inspired by the extensive, systematic dynamic experiments performed by Carr et al. has produced the following conclusions.

1) The constant time-lag approximation of the Karman-Sears wake lag applies to all dynamic stall occurrences, including stall during oscillations in pitch.

2) Adding the moving separation point effect to the quasisteady separation value correctly predicts the "spilling" of the leading-edge vortex.

3) Adding further the time required for the spilled vortex to reach the trailing edge correctly predicts when the peak pitching moment occurs. Whereas the average speed with which the spilled vortex travels from the leading edge to the trailing edge is 55% of freestream velocity for the NACA-0012 and cambered airfoils, as expected, the measurements by Carr et al. indicate that it is only 40% for the sharp leading-edge airfoil.

4) Adding to the previously developed unsteady time equivalent to Polhamus' leading-edge suction analogy the initial growth period for the "spilled" leading-edge vortex, as described by Carta's detailed unsteady pressure measurements, provides analytical means for prediction of the normal force and moment peaks generated by the "spilled" leading-edge vortex.

References

[1] Halfman, R.L., Johnson, H.C., and Haley, S.M., "Evaluation of High-Angle-of-Attack Aerodynamic-Derivative Data and Stall-Flutter Prediction Techniques," TN 2533, 1951, NACA.

[2] Ericsson, L.E. and Reding, J.P., "Dynamic Stall Simulation Problems," *Journal of Aircraft*, Vol. 8, July 1971, pp. 579-583.

[3] Moss, G.F. and Murdin, P.M., "Two-Dimensional Low-Speed Tunnel Tests on the NACA 0012 Section Including Measurements Made During Pitch Oscillation at the Stall," CP No. 1145, Aeronautical Research Council, Great Britain, 1971.

[4] Gregory, N., Quincey, V.G., O'Reilly, C.L., and Hall, D.J., "Progress Report on Observations of Three-Dimensional Flow Patterns Obtained During Stall Development on Airfoils, and the Problem of Measuring Two-Dimensional Characteristics," CP No. 1146, Aeronautical Research Council, Great Britain, 1971; also, NPL Aero Report 1309, 1969.

[5] McCroskey, W.J., "The Inviscid Flowfield of an Unsteady Airfoil," *AIAA Journal*, Vol. 11, Aug. 1973, pp. 1130-1137.

[6] McCroskey, W.J., "Recent Developments in Dynamic Stall," *Proceedings of Symposium on Unsteady Aerodynamics*, University of Arizona, Tucson, Ariz., Vol. 1, March 1975, pp. 1-33.

[7] Ericsson, L.E. and Reding, J.P., "Scaling Problems in Dynamic Tests of Aircraft-Like Configurations," *AGARD Symposium on Unsteady Aerodynamics*, Ottawa, Canada, AGARD CP-227, Paper 25, Sept. 1977.

[8] Ericsson, L.E. and Reding, J.P., "Unsteady Airfoil Stall, Review and Extension," *Journal of Aircraft*, Vol. 8, Aug. 1971, pp. 609-616.

[9] Ericsson, L.E. and Reding, J.P., "Dynamic Stall of Helicopter Blades," *American Helicopter Society Journal*, Vol. 17, Jan. 1972, pp. 10-19.

[10] Ericsson, L.E. and Reding, J.P., "Dynamic Stall Analysis in Light of Recent Numerical and Experimental Results," *Journal of Aircraft*, Vol. 13, April 1976; see also AIAA Paper 75-26, Jan. 1975.

[11] Ericsson, L.E. and Reding, J.P., "'Spilled' Leading Edge Vortex Effects on Dynamic Stall Characteristics," *Journal of Aircraft*, Vol. 13, April 1976, pp. 313-315.

[12] Ericsson, L.E. and Reding, J.P., "Further Consideration of 'Spilled' Leading Edge Vortex Effects on Dynamic Stall," *Journal of Aircraft*, Vol. 14, June 1977, pp. 601-603; errata, *Journal of Aircraft*, Vol. 15, Jan. 1978, p. 64.

[13] Carr, L.W., McAlister, K.W., and McCroskey, W.J., "Analysis of the Development of Dynamic Stall Based on Oscillating Airfoil Experiments," NASA TN D-8382, Jan. 1977.

[14] Liiva, J., Davenport, F.J., Gray, L., and Walton, I.C., "Two-Dimensional Tests of Airfoils Oscillating Near Stall," Vols. I and II, USAAVLABS TR 68-13 A&B, April 1968.

[15] Von Karman, Th. and Sears, W.R., "Airfoil Theory for Non-Uniform Motion," *Journal of Aeronautical Sciences*, Vol. 5, No. 10, Aug. 1938, pp. 370-390.

[16] Ericsson, L.E., "Dynamic Effects of Shock-Induced Flow Separation," *Journal of Aircraft*, Vol. 12, Feb. 1975, pp. 86-92.

[17] Philippe, J.J., "Le Decrochage Instationnaire d'un Profil," TP No. 936, ONERA, 1938.

[18] Werlé, H. and Armand, C., "Measures des Visualisations Instationnaires sur les Rotors," TP No. 777, ONERA, 1969.

[19] Ericsson, L.E. and Reding, J.P., "Analytic Prediction of Dynamic Stall Characteristics," AIAA Paper 72-682, June 1972.

[20] Hurley, D.G. and Ward, G.F., "Experiments on the Effects of Airjets and Surface Roughness on the Boundary Layer Near the Nose of a NACA 64-006 Airfoil," ARL Aero Note 128, Sept. 1963, Aer. Research Labs, Australia.

[21] McCroskey, W.J., Carr, L.W., and McAlister, K.W., "Dynamic Stall Experiments on Oscillating Airfoils," *AIAA Journal*, Vol. 14, Jan. 1976, pp. 57-63.

[22] Ericsson, L.E. and Reding, J.P., "Unsteady Airfoil Stall and Stall Flutter," NASA CR-111906, June 1971.

[23] Carta, F.O., "Analysis of Oscillatory Pressure Data Including Dynamic Stall Effects," NASA CR-2394, May 1974.

[24] Silcox, R.J. and Szwarc, W.J., "Wind Tunnel Dynamic Analysis of an Oscillating Airfoil," AIAA Paper No. 74-259, January 1974.

[25] Philippe, J.J., "Le Decrochage Dynamique: Un Example d'Interaction Forte Entre Ecoulements Visqueaux et NonVisqueaux," *AGARD Symposium on Unsteady Aerodynamics*, Ottawa, Canada, AGARD CP-227, Paper 21, Sept. 1977.

[26] Liiva, J. and Davenport, F.J., "Dynamic Stall of Airfoil Sections for High-Speed Rotors," *Proceedings 24th Annual Forum of the American Helicopter Society*, Washington, D.C., May 1968, Paper No. 206.

[27] Ham, N.D. and Garelick, M.S., "Dynamic Stall Considerations in Helicopter Rotors," *American Helicopter Society Journal*, Vol. 13, April 1968, pp. 44-55.

[28] Ericsson, L.E. and Reding, J.P., "Quasi-Steady and Transient Dynamic Stall Characteristics," Paper 24, AGARD CP-204, AGARD Symp. on Pred. of Aero. Loading, Moffet Field, Calif., Sept. 1976.

[29] Lambourne, N.C., "Some Instabilities Arising from the Interaction Between Shock Waves and Boundary Layers," CP 473, Aeronautical Research Council, Great Britain, Feb. 1958.

[30] McCroskey, W.J. and Philippe, J.J., "Unsteady Viscous Flow on Oscillating Airfoils," AIAA Paper 74-182, Jan. 1974.

[31] Ericsson, L.E. and Reding, J.P., "Dynamic Stall Analysis in Light of Recent Numerical and Experimental Results," AIAA Paper 75-26, Jan. 1975.

[32] McCroskey, W.J., "Prediction of Unsteady Separated Flows on Oscillating Airfoils," AGARD Lecture Series on Three-Dimensional and Unsteady Separated Flow at High Reynolds Numbers, VKI, Belgium, AGARD LS-94, Paper 12, Feb. 1978.

[33] Bore, C.L., "Unsteady Airloads in Separated and Transonic Flow," AGARD SMP Specialists' Meeting on Unsteady Airloads in Separated and Transonic Flow, Lisbon, Portugal, AGARD-CP-226, Paper 1, April 1977.